

DOT HS-801 247

# **TWO PROBLEMS IN TIRE SHEAR FORCE EVALUATION:**

**The Influence of Wheel Deceleration Rate  
on Braking Force and A Methodology for Obtaining  
Tire Side Force Numerics**

**Contract No. DOT-HS-031-3-676**

**October 1974**

**Final Report**

**PREPARED FOR:**

**U.S. DEPARTMENT OF TRANSPORTATION  
NATIONAL HIGHWAY TRAFFIC SAFETY ADMINISTRATION  
WASHINGTON, D.C. 20590**

This document is disseminated under the sponsorship of the Department of Transportation in the interest of information exchange. The United States Government assumes no liability for its contents or use thereof.

1. Report No. DOT HS-801 247		2. Government Accession No.		3. Recipient's Catalog No.	
4. Title and Subtitle Two Problems in Tire Shear Force Evaluation: (1) The Influence of Wheel Deceleration Rate on Braking Force, (2) A Methodology for Obtaining Tire Side Force Numerics				5. Report Date October 1974	
7. Author(s) R. E. Wild, J. T. Tielking, P.S. Fancher				6. Performing Organization Code	
9. Performing Organization Name and Address Highway Safety Research Institute The University of Michigan Huron Parkway & Baxter Road Ann Arbor, Michigan 48105				8. Performing Organization Report No. UM-HSRI-PF-74-8	
12. Sponsoring Agency Name and Address Safety Research Laboratory National Highway Traffic Safety Administration U.S. Department of Transportation Washington, D.C. 20590				10. Work Unit No.	
				11. Contract or Grant No. DOT-HS-031-3-676	
				13. Type of Report and Period Covered Final Report June 1973-June 1974	
15. Supplementary Notes					
16. Abstract This report deals with (1) the influence of wheel deceleration rate on the braking force produced by pneumatic tires and (2) numerics for evaluating the lateral force performance of pneumatic tires. It is found that the maximum braking force obtained from passenger car tires operated on wet surfaces can be significantly affected by wheel deceleration rate.  Three numerics have been chosen to provide a safety-relevant condensation of tire lateral force data. These numerics are (1) cornering stiffness at rated load and inflation pressure, (2) maximum lateral force at 40 mph on representative wet surfaces and (3) the rate of change of maximum lateral force evaluated at 40 mph on the same wet surfaces.					
17. Key Words Tire Traction, Tire Braking Force, Tire Lateral Force, Tire Grading				18. Distribution Statement Document is available to the public through the National Technical Information Service, Springfield, Virginia 22151	
19. Security Classif. (of this report) Unlimited		20. Security Classif. (of this page) Unlimited		21. No. of Pages 45	22. Price



## TABLE OF CONTENTS

INTRODUCTION. . . . .	1
PART I: THE INFLUENCE OF WHEEL DECELERATION RATE ON BRAKING FORCE. . . . .	3
1.1 Results of the Literature Survey . . . . .	3
1.2 Experimental Investigation . . . . .	4
REFERENCES. . . . .	17
APPENDIX 1: HSRI MOBILE TIRE TESTER. . . . .	18
APPENDIX 2: ASTM TIRE SKID NUMBERS . . . . .	22
APPENDIX 3: TEST RESULTS . . . . .	23
APPENDIX 4: EXAMPLE OF STATISTICAL PROCEDURES EMPLOYED USING DATA FROM TIRE AM-17 ON CONCRETE . . . . .	28
PART II: TIRE-TRACTION GRADING NUMERICS DESCRIPTIVE OF TIRE SIDE-FORCE CHARACTERISTICS . . . . .	33
2.1 Cornering Stiffness, $C_{\alpha}$ . . . . .	33
2.2 Maximum Lateral Force and Its Sensitivity to Velocity. . . . .	35
2.3 Interpretation of Lateral Traction Quality Grading Numerics . . . . .	39
REFERENCES. . . . .	45



## INTRODUCTION

This report presents the results and findings obtained in a research study entitled "Two Problems in Tire Shear Force Evaluation: (1) The Influence of Wheel Deceleration Rate on Braking Force and (2) A Methodology for Obtaining Tire Side Force Numerics." This study was completed by the Highway Safety Research Institute (HSRI) of The University of Michigan for the Safety Research Laboratory (SRL) of the National Highway Traffic Safety Administration.

Each of the problems referred to in the title of this study is related to the general problem of quantifying tire shear-force performance. Nevertheless, these two problems represent distinctly different technical challenges. Consequently, they have been treated separately in this project. Accordingly, this report is divided into two parts entitled: "Part I, The Influence of Wheel Deceleration Rate on Braking Force" and "Part II, Tire-Traction Grading Numerics Descriptive of Tire Side-Force Characteristics."

The principal finding of the study of the influence of wheel deceleration rate on braking force is that the maximum braking force produced by passenger car tires on wet-road surfaces can be significantly affected by wheel deceleration rate. This finding derives from test results obtained with the HSRI mobile tire tester. A search of the literature has revealed that no experimental results have been published comparable to the data obtained in this test program. Thus, this study appears to be unique.

In Part II, three numerics are chosen to provide a rational condensation of free-rolling lateral tire force data. These numerics are: (1) cornering stiffness,  $C_{\alpha}$ , (2) maximum lateral force, MLF, and (3) the rate of change of MLF with respect to velocity.

The cornering stiffness numeric was selected because of its importance to directional control in normal driving. The maximum lateral force (MLF) and the rate of change of MLF with respect to velocity are picked to define the limit of tire traction on wet surfaces, a limit which is known to be velocity sensitive. No scheme was found whereby a single numeric was felt to be sufficient to grade tire traction on wet surfaces for speeds from 20 to 55 mph. Consequently, two numerics, MLF at 40 mph and the rate of change of MLF with respect to velocity at 40 mph, have been chosen. All three of these numerics are found to be independent of each other.

These findings are presented and discussed in detail in Parts I and II, respectively, which follow.



## PART I

### THE INFLUENCE OF WHEEL DECELERATION RATE ON BRAKING FORCE

The subject investigation consisted of two tasks—a literature survey and an experimental study. The findings obtained in each task are presented below.

#### 1.1 RESULTS OF THE LITERATURE SURVEY

The following subject headings were examined in the card catalog of the HSRI library\*: tire longitudinal force, tire braking force, tire dynamics, tire friction, tire traction, tire mechanics, tire shear force, antilocking brake systems, and anti-skid brake controls.

Of the approximately 450 document titles under these subject headings, 54 were selected for reading. These documents were chosen (on the basis of their titles) as possibly containing some research into the effects of wheel angular deceleration on braking force as a part of their major topic. No paper was found that dealt specifically with the desired subject. Of the 54 papers read, only three contained any statement referring to lock-up rate, and none of these were quantitative.

These three statements are: "No stabilized platform was used for the decelerating vehicle nor was the braking rate optimized." [1]; "To allow the measuring decelerometer to respond to the transient maximum deceleration occurring prior to wheel lock the brakes must be applied slowly, in a controlled manner." [2]; "Approach test surface at speed slightly higher than test speed, shift to neutral, turn on recorder, and then apply front brakes slowly (1/2 to 1 second to lockup) until front wheels lock at test speed." [3]. In addition, Reference [1] refers to "rate of brake lock-up" as a source of experimental error in measuring braking traction by means of either vehicle or trailer testing.

---

\*A library containing more than 30,000 documents related to highway safety and which endeavors to maintain an exhaustive collection in the area of tire mechanics.

The above remarks indicate that wheel angular deceleration is sometimes considered in a test plan. Indeed, the implication in Reference [1] is that the author has experienced data variability due to varying rates of wheel lock-up. In summary, however, the literature survey produced no direct information on the effects of wheel angular deceleration on braking force.

## 1.2 EXPERIMENTAL INVESTIGATION

1.2.1 MEASUREMENT PROCEDURE. The test program consisted of gathering peak braking force data on six different tires on three wetted surfaces at five different linear rates of lock-up (i.e., rate of change of longitudinal slip). Eight to ten replications were made at each lock-up rate. The specific test conditions are tabulated below:

Measurement Device: HSRI mobile tire tester (a description and calibration data are contained in Appendix I)

Tires: The six tires provided by SRL are listed below:

<u>SRL Code #</u>	<u>Size</u>	<u>Rim</u>	<u>Load</u>	<u>PSI</u>	<u>Manufacturer's Nomenclature</u>
AM-17	G78-15	15 x 6	1150	24	Goodyear Custom Power Cushion Polyglas
CM-17	205R-15	15 x 6	1150	24	Sears Allstate Radial
BM-13	G78-15	15 x 6	1150	24	Firestone 500 78 Polyester
ZM-5	750-14	14 x 5	1100	24	Previous ASTM standard tire (fabricated by General Tire)
AM-19	G60-15	15 x 7	1150	24	Goodyear Custom Widetread Polyglas GT
FM-3	8.0/28.0 x 15	15 x 6	1150	24	M&H Racemaster Drag Slick Compound 330

Surfaces: Three 24' x 600' "skid pads" located at the Texas Transportation Institute. These "pads" consisted of a Portland cement concrete surface ( $SN_{40} = .40^*$ ), a jennite covered asphalt surface ( $SN_{40} = .13^*$ ) and a crushed gravel hot mix (called asphalt in this report) ( $SN_{40} = .47^*$ ).

Speed: 40 mph

Water Depth: .02 inch (as obtained from a calculated delivery of on-board water)

Nominal Lock-up Times (i.e., times required to linearly traverse from 0 to 100% longitudinal slip): .5, .8, 1.2, 2.4 seconds and a fixed longitudinal slip condition lasting approximately seven seconds\*\*

(Because of the widely varying demands placed on the hydraulic drive system by different tire-pavement combinations, the measured lock-up times, as determined from the oscillograph recording, were usually considerably different from these nominal values. The times obtained for the replications within each individual tire-pavement combination, however, were consistent to  $\pm .02$  second.)

A complete set of measurements on one tire was made within a 2- or 3-hour time span by proceeding from the fastest lock-up rate to the slowest, obtaining the desired number of replications at each rate.

---

\*These skid numbers were obtained by the mobile tire tester, using tire ZM-5, an old-style ASTM standard tire. The skid number data are presented in Appendix 2.

\*\*Tests were conducted at approximately six different values of fixed longitudinal slip with the data being plotted to discern the maximum braking force produced under steady slip conditions.

1.2.2 DATA ANALYSIS PROCEDURES. The values of maximum braking force,  $F_{x_i}$ , obtained for each tire-pavement-lock-up rate combination were analyzed to yield the value,  $\bar{F}_x$ , the standard deviation,  $\hat{\sigma}$ , and the standard deviation of the mean,  $\hat{\sigma}_m$ . The standard deviation was computed according to

$$\hat{\sigma} = \sqrt{\frac{\sum_{i=1}^n (F_{x_i} - \bar{F}_x)^2}{n-1}}$$

where

$n$  = number of replications at each test condition.

The standard deviation of the mean (frequently called the "standard error") was calculated from

$$\hat{\sigma}_m = \frac{\hat{\sigma}}{\sqrt{n}}$$

It should be recalled that if a new mean were to be obtained from additional testing, there is a 95% probability that it will fall in a band  $\pm 2\hat{\sigma}_m$  centered about the previous mean.

The above quantities were not calculated for the steady-state data; rather, temporal averages were determined. The values of  $\bar{F}_x$ ,  $\hat{\sigma}$ , and  $\hat{\sigma}_m$  for all tire-pavement-rate combinations are contained in Appendix 3.

Inspection of the data presented in Appendix 3 shows that different rates of angular deceleration yielded different values of  $\bar{F}_x$  for the same tire-pavement combination. It is possible, however, that many of these observed differences are simply due to the random variations in the individual values of  $F_{x_i}$  making up each mean, rather than being due to the different experimental "treatments" (lock-up times). Accordingly, an analysis of variance (ANOVA) was employed to show which of the groups of  $\bar{F}_x$

contained mean values that were too widely separated to be attributable to random error. ANOVA is a statistical procedure which compares the variation among means resulting from different experimental treatments to the variation among the individual values within each treatment.

One of the assumptions underlying the ANOVA procedure is that the population variances are equal. Therefore, it is advisable to test for homogeneity of variance prior to using ANOVA. Inspection of the values of  $\hat{\sigma}$  in Appendix 3 shows that the sample variances for each tire-pavement combination are not numerically equal (variance =  $\hat{\sigma}^2$ ). However, these sample variances are only estimates of the true population variances. Cochran's statistic [4], viz,

$$C = \frac{\hat{\sigma}_{\max}^2}{4 \sum_{j=1}^4 \hat{\sigma}_j^2}$$

where

$$\hat{\sigma}_{\max} = \text{maximum of } \hat{\sigma}_j \text{ for } j=1, \dots, 4$$

was used to test the hypothesis that the four population variances for each tire-pavement combination were equal at the 0.05 level of significance. None of the hypotheses could be rejected on the basis of Cochran's test. Therefore, the four population variances in each tire-pavement combination were assumed equal, and the ANOVA procedure was carried out using the standard F statistic [4] at the 0.05 level of significance, viz:

$$\begin{aligned} F_{k-1, N-k, .05} &= \frac{\text{variation among sample means}}{\text{variation within individual samples}} \\ &= \frac{MS_2}{MS_1} \end{aligned}$$

where

k = the number of treatments (lock-up times) = 4

N = the total number of observations = n·k

n = the number of observations per treatment

$$MS_2 = n \cdot \frac{\sum_{j=1}^k (\bar{x}_j - \bar{x})^2}{k - 1}$$

where

$\bar{x}_j$  = sample mean

$\bar{x}$  = grand mean

and

$$MS_1 = \frac{\sum_{j=1}^k \sum_{i=1}^n (x_{ji} - \bar{x}_j)^2}{k(n-1)} = \frac{\sum_{j=1}^k \delta_j^2}{k} \quad *$$

where

$x_{ji}$  = individual test result

The results of the analysis of variance are contained in Table 1. Note that statistically significant differences exist between mean values of peak braking force for different lock-up rates for most tire-pavement combinations.

---

\*The simplification to  $MS_1 = \frac{\sum_{j=1}^k \delta_j^2}{k}$  cannot be made for cases

where  $n_1 = n_2 = \dots n_k$  is not true.

TABLE 1  
RESULTS OF ANOVA

(X means data passed F test, no significant differences  
between mean values; F means data failed F test,  
significant differences exist)

	<u>Concrete</u>	<u>Jennite</u>	<u>Asphalt</u>
AM-17	F	F	F
AM-19	F	F	F
BM-13	F	F	F
CM-17	F	X	F
FM-3	X	X	X
ZM-5	X	X	F

A closer examination of Table 1 indicates that a correlation may exist between tread pattern and the influence of lock-up rate. The maximum braking force of the tire with no tread pattern, i.e., FM-3, was not affected by changes in lock-up rate on any surface. The maximum braking force of tire ZM-5, which has circumferential ribs but no sipes or kerfs, was affected by lock-up rate only on the coarsest surface. The tires with normal tread patterns generally exhibited an influence of variation in lock-up rate on maximum braking force.

The ANOVA procedure merely establishes which tire-pavement combinations were affected by lock-up rate. A second analysis procedure is necessary to establish the minimum significant differences between the values of  $\bar{F}_x$  within each tire-pavement combination selected by ANOVA. The Newman-Keuls procedure [4] was chosen to compute these minimum significant differences. An example of the entire statistical process employed (Cochran, ANOVA, Newman-Keuls), using the data from tire AM-17 on concrete, is contained in Appendix 4. The results obtained using these procedures are summarized below.

In Table 2, the numbers 1-5 represent the nominal lock-up times in increasing order of lock-up time, i.e., 1 = shortest time (.5 sec.) and 5 = longest time (steady-state). Lock-up times underlined by a common line produced mean values of maximum braking force that did not differ in a statistically significant manner; times not underlined by a common line did produce statistically different results. In general, the lock-up times for each tire-pavement combination fall into only two groups, rather than each rate producing a distinctly different result. A plot of the data utilized in the Newman-Keuls procedure is presented in Figure 1a through 1e, together with the results of the Newman-Keuls analysis as displayed in Table 2. Note that the vertical bars represent variations of  $\pm 2\hat{\sigma}_m$  about the mean values.

TABLE 2

	<u>Concrete</u>	<u>Jennite</u>	<u>Asphalt</u>
AM-17	1 <u>2 3 4 5</u>	<u>4 5</u> <u>1 2 3</u>	<u>1 2</u> <u>3 4 5</u>
AM-19	<u>2 1 3 4 5</u>	<u>1 2 3 4 5</u>	<u>1 2 3</u> <u>4 5</u>
BM-13	<u>5 4 3</u> 2 1	<u>5 4 3 2</u> 1	<u>5 4 3 2</u> 1
CM-17	<u>3 2 4 5</u> 1	X	<u>3 2 4 5</u> 1
FM-3	X	X	X
ZM-5	X	X	<u>1 2 3 4 5</u>

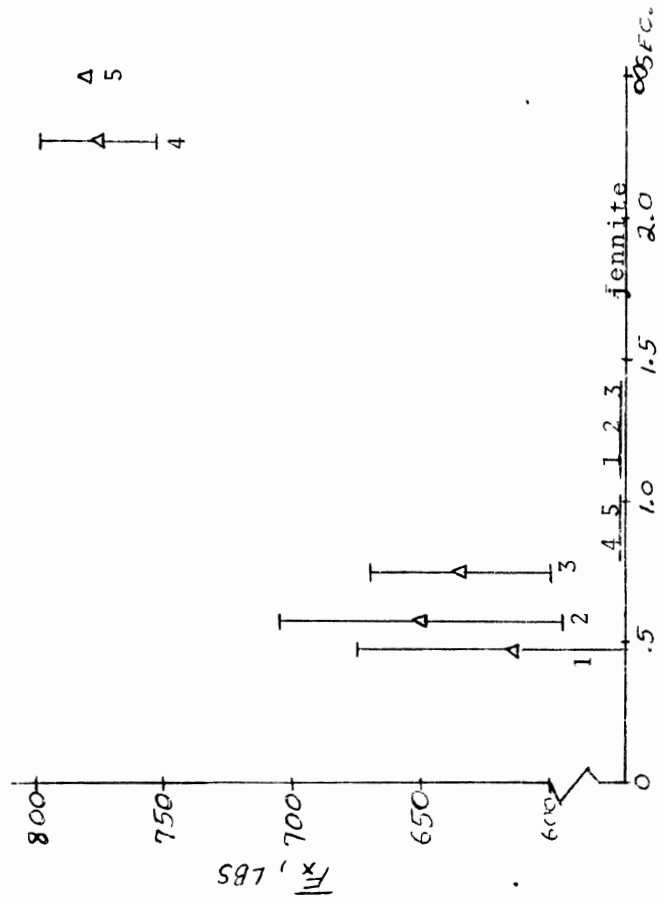
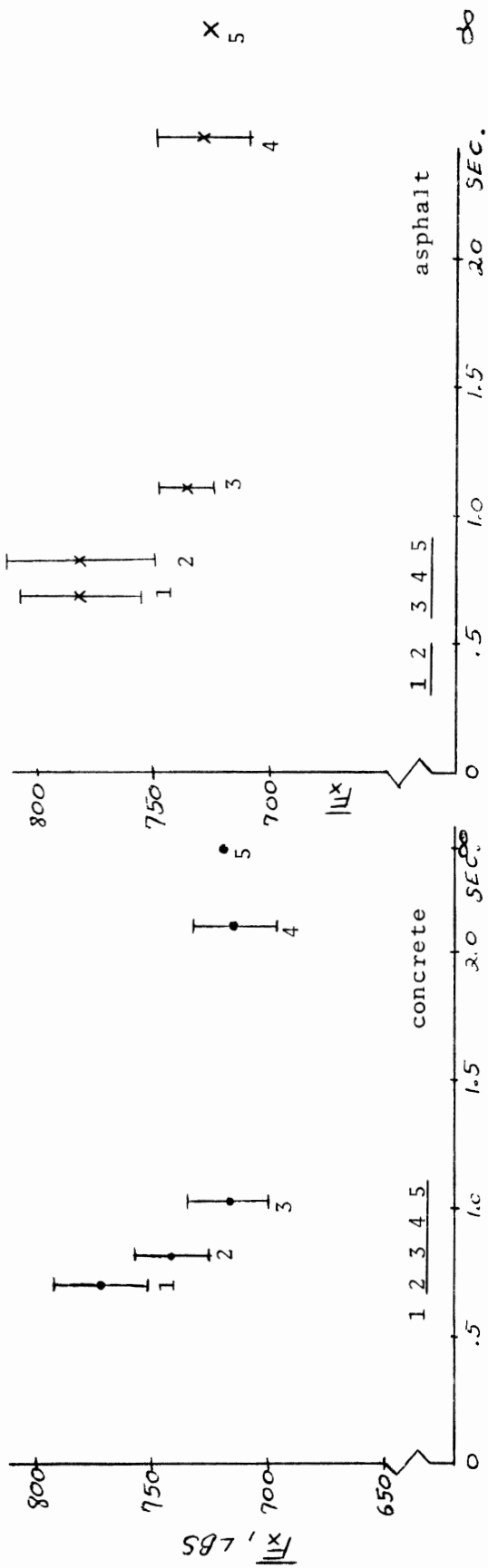
1.2.3 DISCUSSION OF RESULTS. It appears that the maximum braking force,  $\bar{F}_x$ , produced by typical passenger car tires (as tested in this program) is influenced by lock-up rate. The magnitude of this effect ranged from about 5% for CM-17 on concrete to about 33% for BM-13 on jennite. However, longer lock-up times led to higher values of  $\bar{F}_x$  for some tire-pavement combinations, while for other combinations, the opposite was true. Thus the results do not lend themselves to producing a generalized finding.



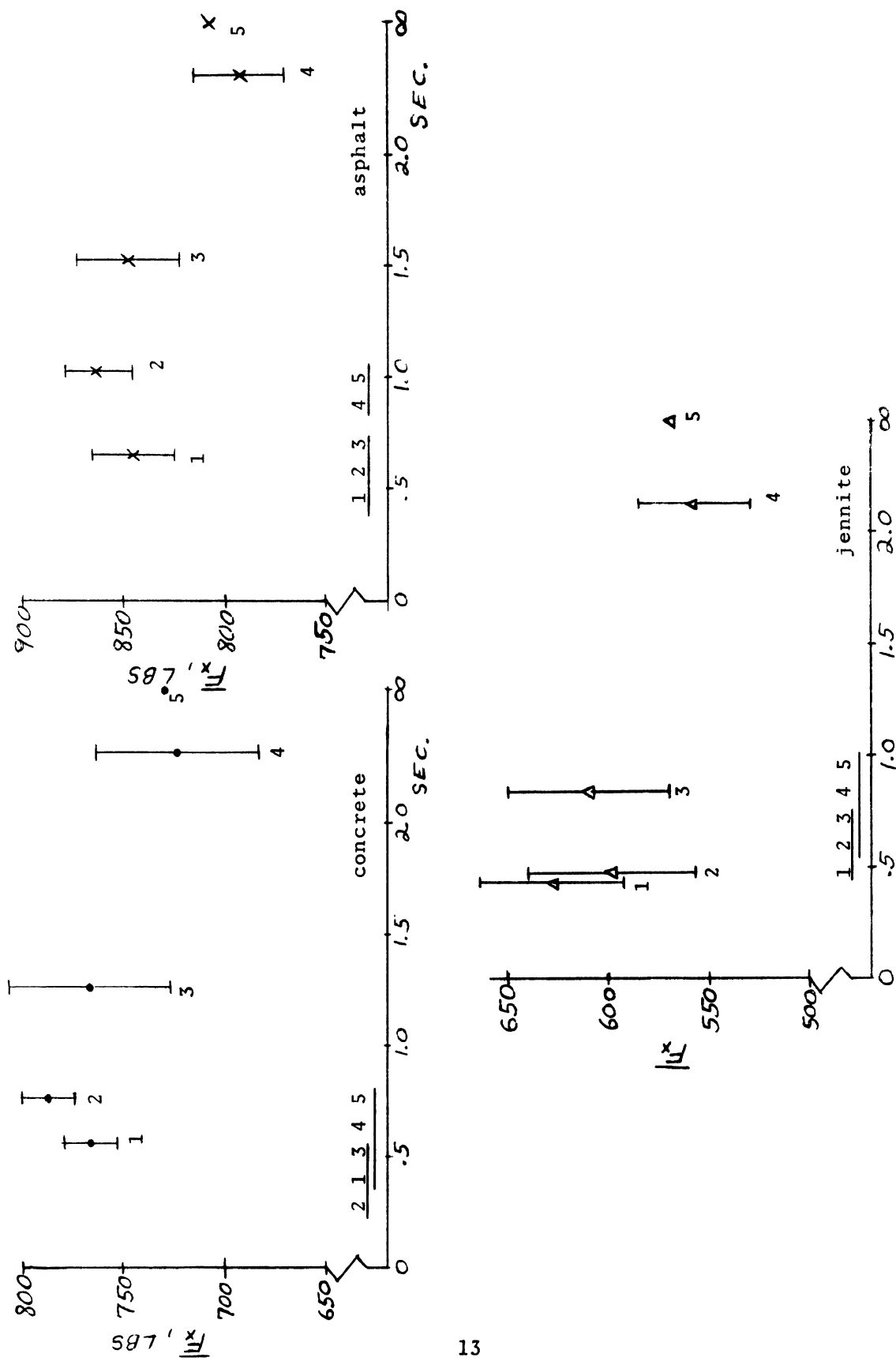
The most consistent finding is that lock-up treatments 4 and 5, the 2.4-second and steady-state results, produced nearly equal values of  $\bar{F}_x$  for all tire-pavement combinations. Also, inspection of Figures 1a-3 shows that the results may order themselves according to tire construction. For example, the bias ply tire, BM-13, exhibited the greatest influence of lock-up rate on maximum braking force; the radial ply tire, CM-17, exhibited the least influence of lock-up rate; the bias-belted designs, AM-17 and AM-19, exhibited an influence whose magnitude was somewhere between those exhibited by the BM-13 (bias ply) and the CM-17 (radial).

The values of  $\bar{F}_x$  resulting from treatment 1, the fastest lock-up rate, were different from the values resulting from treatments 4 and 5 for tires AM-17, AM-19, and BM-13. Tire CM-17 exhibited a "peaking" phenomenon wherein the value of  $\bar{F}_x$  produced by an intermediate value of lock-up rate, treatment 3, was above that produced by either faster or slower rates on asphalt and concrete. In 7 of the 12 entries in Table 2, significant differences exist in the values of  $\bar{F}_x$  that are produced by lock-up times of .5 and 1.2 seconds, a range of lock-up times that very likely occur in making braking force measurements.

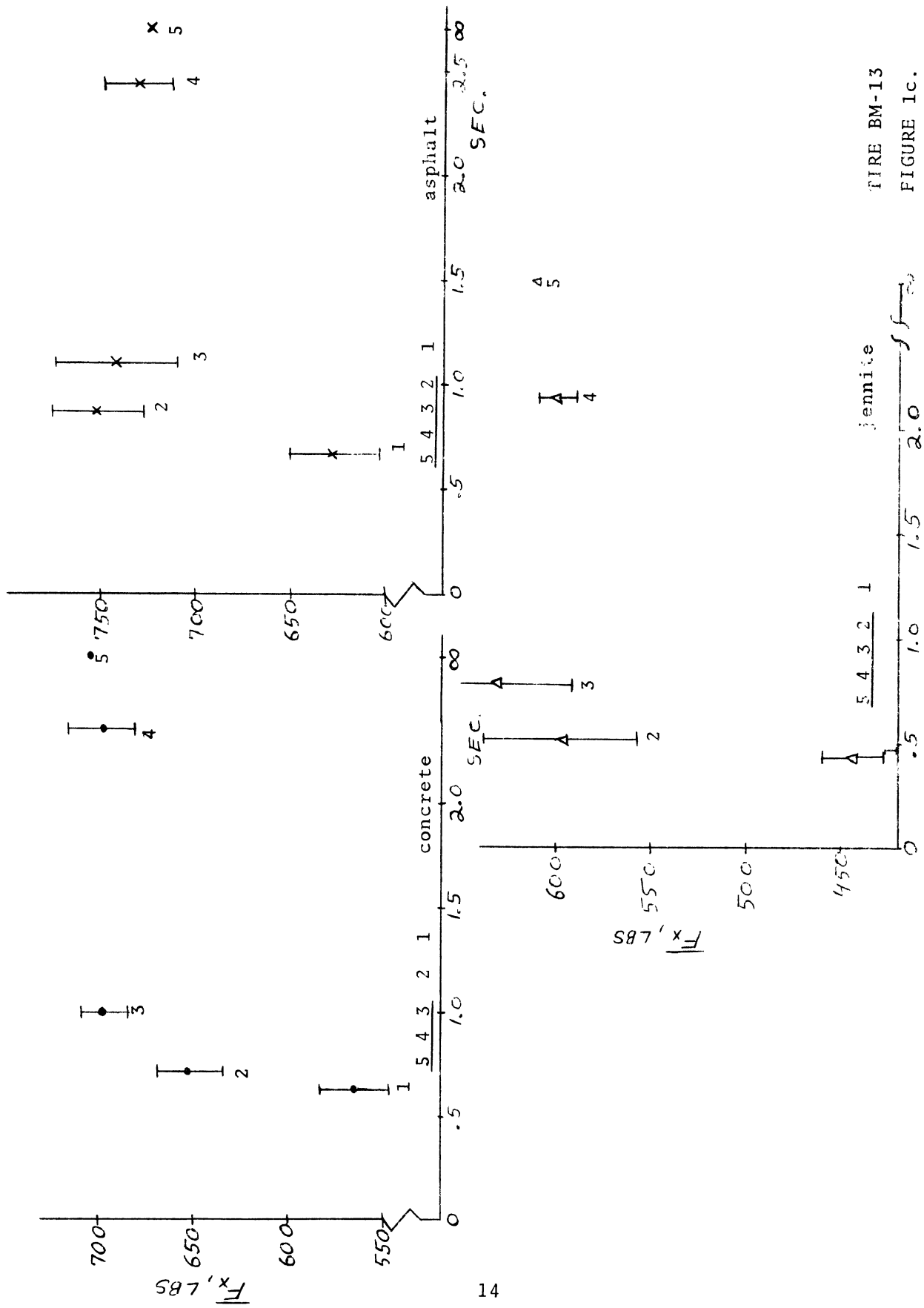
In summary, the results of this experimental program show that mean values of maximum braking force generated by passenger car tires on wet road surfaces can be significantly affected by wheel angular deceleration rate. On the other hand, it is not possible to quantify this statement in view of the rather small amount of data collected in this study. Much more data needs to be collected and analyzed if the effects of wheel angular deceleration are to be well defined. It appears, however, that lock-up rate is a variable to be reckoned with in test programs seeking to measure the maximum or "peak" braking force. Clearly, if measurements of maximum braking force were to be included in the tire traction quality grading standards, the effects of lock-up rate would assume major importance.



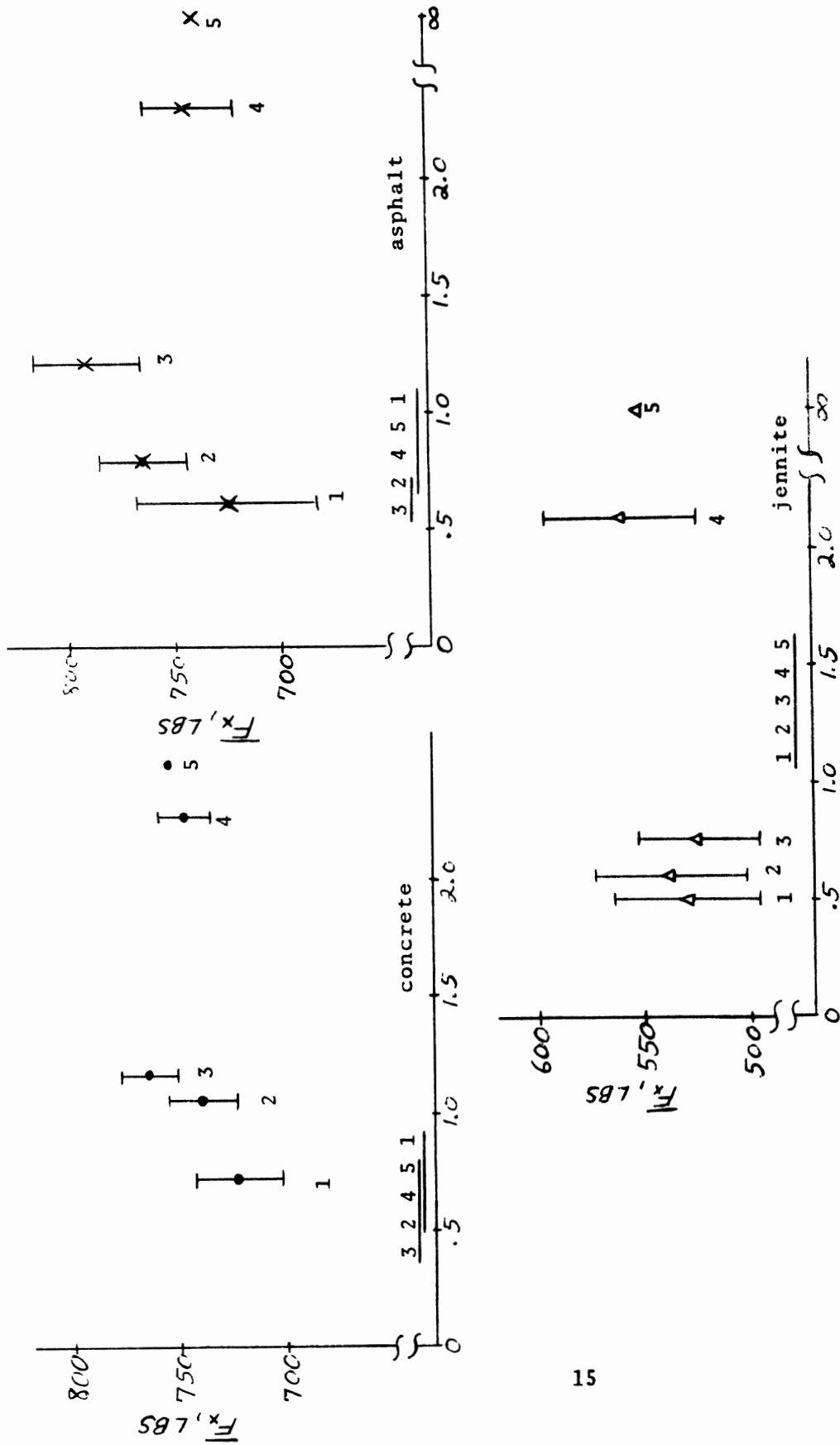
TIRE AM-17  
FIGURE 1a.



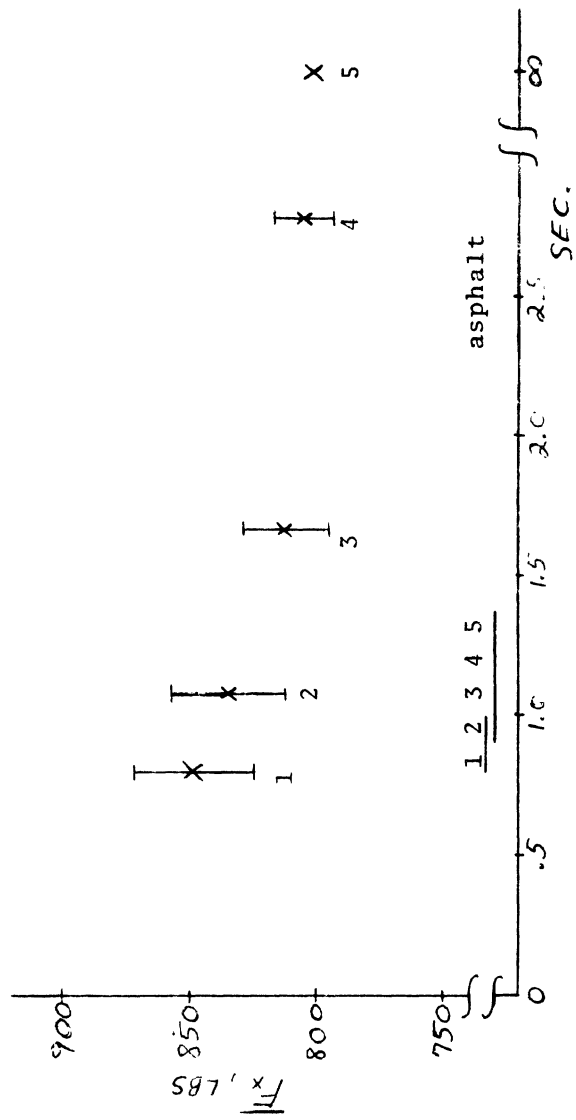
TIRE AM-19  
FIGURE 1b.



TIRE BM-13  
FIGURE 1c.



TIRE CM-17  
FIGURE 1d.



TIRE ZM-5

FIGURE 1e.

## REFERENCES

1. Spelman, R.H., et al., "SAE Study - Wet Pavement Braking Traction," SAE Paper #700462.
2. Bajer, J.J., "Proposal for a Procedure for Evaluating Wet Skid Resistance of a Road-Tire-Vehicle System," SAE Paper #690526.
3. Smithson, F.D., "Vehicle Test Method for Measuring Tire-Road Braking Traction Characteristics," General Motors Engineering Publication A-2713, April 1971.
4. Winer, B.J., Statistical Principles in Experimental Design, Second Ed., McGraw-Hill Book Company, 1962.

## APPENDIX 1

### HSRI MOBILE TIRE TESTER

The HSRI mobile tire tester consists of a retractable test wheel mounted on the rear of a modified tandem-axle commercial tractor (shown on the next page) which serves as the test bed. The test wheel accommodates tires in a size range 6.45-14 to 9.15-15. A dead-weight vertical tire load (independent of the test bed) in the range 600 to 2000 lb. may be used. The test wheel is attached to the test bed through a transducer sensitive to longitudinal and lateral tire forces and aligning moment. Calibration tests show transducer accuracy to be approximately  $\pm 1.5$  percent of full scale as calibrated "on truck," under all conditions of loading.

The on-board data acquisition system, consisting of an FM magnetic tape recorder and a light-beam oscillograph, is mounted in the sleeper portion of the tractor cab along with test wheel control instrumentation. Electrical power for the instrumentation is supplied by an on-board gasoline-fueled 6.4 KW AC generator. Other test data recorded are tread surface temperature (from an infrared radiometer mounted above the test tire), test wheel angular velocity, and test bed velocity. These last two quantities yield a precise measure of test tire longitudinal slip.

The test wheel is driven by a hydraulic motor which allows test wheel speed to be varied independently of test bed speed. The hydraulic motor is controlled from the cab and operates in three modes: steady-state (constant) slip, slip varying linearly with time, and sinusoidal slip variation with time. The last two modes are controlled by automatic programs to cycle the longitudinal slip between adjustable limits in an adjustable time span.



Either braking or driving torque is developed by driving the test wheel at a rotational rate corresponding to a linear velocity less than or greater than that of the test bed. This method of generating braking torque has several advantages over braking by a conventional mechanical brake (drum or disc). A tire controlled by a mechanical brake exhibits extremely rapid lock-up after developing its peak braking force and the data is prone to spurious transients. The mobile tire tester is able to control test wheel acceleration and deceleration over the entire longitudinal slip range of tire operation (driving to free-rolling to locked wheel).

The performance characteristics of the mobile tire tester are tabulated below:

TEST BED (International Harvester COF 4000 diesel)

Wheelbase	= 142 in.
Net hp	= 300 at 2100 rpm
Gross hp	= 318 at 2100 rpm
Max. GVW	= 45,000 lb
Max. speed	= 70 mph
Total present weight	= 23,687 lb

TEST WHEEL SPECIFICATIONS

Max. vertical load	= 2000 lb
Max. braking torque	= 1500 ft. lbs.
Max. steer angle	= 20° (can be increased to 26° with certain modifications)

LONGITUDINAL SLIP CONTROL SYSTEM

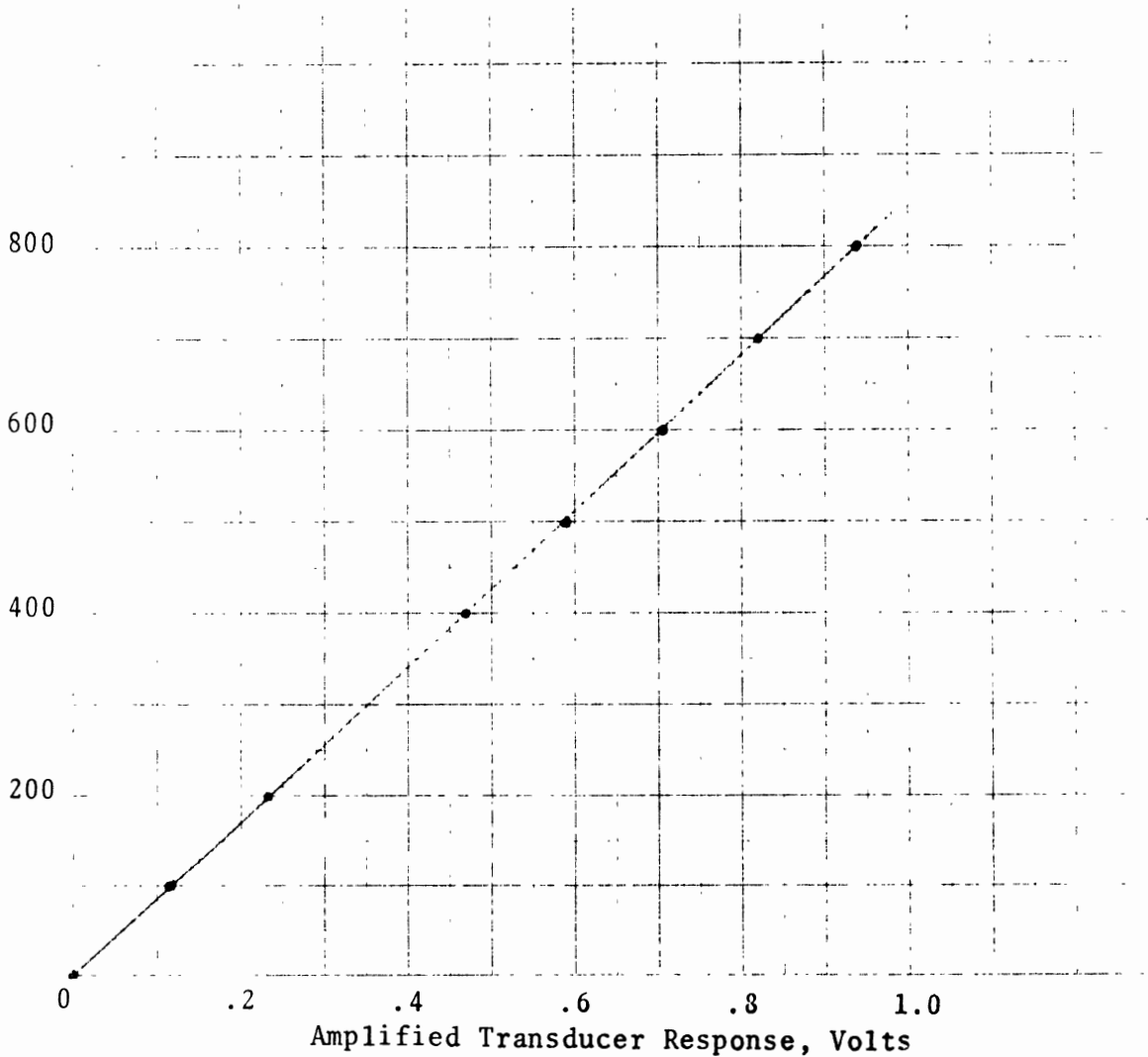
Hydreco Model 110 variable displacement pump driving a Hydreco motor capable of generating 190 hp (e.g.,  $F_x = 1000$  lb at 70 mph). (This system will drive the test wheel at 0% wheel slip at 55 mph or, at 45 mph, the test wheel may be driven at -30% slip, thereby producing a driving force rather than a braking force.)

A steady-state lateral slip is achieved by presetting the tire-transducer assembly to a steer angle relative to the test bed. Longitudinal slip, via the hydraulic motor, can be applied or the drive shaft disconnected from the test wheel for performing free-rolling lateral force measurements. A measurement of rolling resistance is obtained by operating the test wheel in a free-rolling mode at zero degree slip angle.

An additional feature is the on-board 540 gal. water tank with a remote-controlled gate valve and road surface delivery system. The flow rate is adjusted with vehicle speed to obtain the amount of water required to produce the desired water depth.

HSRI Mobile Tire Tester Braking Force  
Calibration Using Federal Highway Admin-  
istration Force Plate at Texas Transpor-  
tation Institute. 1200 Pounds Vertical  
Load, February 19, 1974.

<u>Data Points</u>	
<u>Calibration Force</u>	<u>Transducer Response</u>
.0 pounds	0 Volts
100	.115
200	.232
400	.469
500	.590
600	.705
700	.820
800	.937



APPENDIX 2  
ASTM TIRE SKID NUMBERS

	<u>Concrete</u>	<u>Jennite</u>	<u>Asphalt</u>
	.40	.12	.46
	.41	.13	.47
	.39	.13	.47
	.42	.16	.47
	.39	.14	.46
	.40	.13	.47
	.40	.14	.46
	.40	.12	.48
$\bar{\mu}$	.401	.133	.467
$\hat{\sigma}$	.0099	.013	.007
$\hat{\sigma}_m$	.0035	.0046	.0025

Note that these values are quite different from those obtained on the same surface by the same device, the mobile tire tester, in February 1972. The 1972 data, using tire ZM-3, is:

$\bar{\mu}$	.47	.10	.39
$\hat{\sigma}$	.024	.025	.027
$\hat{\sigma}_m$	.007	.007	.008

The concrete and asphalt surfaces have changed considerably in the intervening two years.

APPENDIX 3  
TEST RESULTS  
MAXIMUM BRAKING FORCE ( $\bar{F}_x$ ) VERSUS LOCK-UP TIME (LT)

Concrete

AM-17

LT	<u>.70 sec</u>	<u>.81 sec</u>	<u>1.03 sec</u>	<u>2.10 sec</u>	<u><math>\infty^*</math></u>
$\bar{F}_x$	773	742	717	715	720
$\hat{\sigma}$	31.91	25.14	26.94	27.09	
$\hat{\sigma}_m$	10.09	7.95	8.52	8.56	
n	10	10	10	10	1

AM-19

LT	<u>.58 sec</u>	<u>.78 sec</u>	<u>1.28 sec</u>	<u>2.31 sec</u>	<u><math>\infty</math></u>
$\bar{F}_x$	768	788	768	724	730
$\hat{\sigma}$	20.07	21.34	51.56	55.93	
$\hat{\sigma}_m$	6.34	6.74	19.49	19.77	
n	10	10	7	8	1

BM-13

LT	<u>.63 sec</u>	<u>.71 sec</u>	<u>1.02 sec</u>	<u>2.36 sec</u>	<u><math>\infty</math></u>
$\bar{F}_x$	566	653	698	698	705
$\hat{\sigma}$	26.58	25.53	17.94	27.54	
$\hat{\sigma}_m$	8.40	8.07	5.98	8.71	
n	10	10	9	10	1

CM-17

LT	<u>.72 sec</u>	<u>1.06 sec</u>	<u>1.17 sec</u>	<u>2.29 sec</u>	<u><math>\infty</math></u>
$\bar{F}_x$	724	740	765	748	755
$\hat{\sigma}$	28.77	23.56	22.26	15.77	
$\hat{\sigma}_m$	9.59	8.33	6.42	5.57	
n	9	8	10	8	1

\*The symbol " $\infty$ " stands for infinite lock-up time and more correctly identifies the maximum braking force that was obtained under fixed or steady slip conditions.

FM-3

LT	<u>.44 sec</u>	<u>.52 sec</u>	<u>.82 sec</u>	<u>2.07 sec</u>	<u><math>\infty</math></u>
$\bar{F}_x$	322	346	331	294	311
$\hat{\sigma}$	33.27	26.62	45.83	33.25	
$\hat{\sigma}_m$	11.09	8.87	16.20	11.75	
n	9	9	8	8	1

ZM-5

LT	<u>.66 sec</u>	<u>.84 sec</u>	<u>1.24 sec</u>	<u>2.74 sec</u>	<u><math>\infty</math></u>
$\bar{F}_x$	758	759	775	769	775
$\hat{\sigma}$	29.93	31.85	13.29	12.18	
$\hat{\sigma}_m$	9.46	10.07	4.70	4.30	
n	10	10	8	8	1

Jennite

AM-17

LT	<u>.47 sec</u>	<u>.58 sec</u>	<u>.74 sec</u>	<u>2.28 sec</u>	<u><math>\infty</math></u>
$\bar{F}_x$	614	650	635	777	782
$\hat{\sigma}$	95.39	90.46	54.32	36.19	
$\hat{\sigma}_m$	30.16	28.60	17.18	11.44	
n	10	10	10	10	1

AM-19

LT	<u>.43 sec</u>	<u>.49 sec</u>	<u>.84 sec</u>	<u>2.12 sec</u>	<u><math>\infty</math></u>
$\bar{F}_x$	629	598	610	559	570
$\hat{\sigma}$	57.39	65.17	55.50	38.34	
$\hat{\sigma}_m$	18.14	20.61	19.62	13.55	
n	10	10	8	8	1

BM-13

LT	<u>.44 sec</u>	<u>.51 sec</u>	<u>.78 sec</u>	<u>2.13 sec</u>	<u>∞</u>
$\bar{F}_x$	444	596	632	601	612
$\hat{\sigma}$	23.67	57.17	46.98	17.42	
$\hat{\sigma}_m$	7.48	19.05	15.66	5.50	
n	10	9	9	10	1

CM-17

LT	<u>.49 sec</u>	<u>.60 sec</u>	<u>.76 sec</u>	<u>2.14 sec</u>	<u>∞</u>
$\bar{F}_x$	531	539	527	561	552
$\hat{\sigma}$	47.39	54.57	39.37	51.79	
$\hat{\sigma}_m$	16.75	17.25	13.92	18.31	
n	8	10	8	8	1

FM-3

LT	<u>.37 sec</u>	<u>.46 sec</u>	<u>.81 sec</u>	<u>2.07 sec</u>	<u>∞</u>
$\bar{F}_x$	119	106	125	99	106
$\hat{\sigma}$	15.95	14.96	23.67	16.38	
$\hat{\sigma}_m$	5.63	4.73	8.94	5.79	
n	8	10	8	8	1

ZM-5

LT	<u>.50 sec</u>	<u>.54 sec</u>	<u>.77 sec</u>	<u>2.55 sec</u>	<u>∞</u>
$\bar{F}_x$	342	349	328	358	350
$\hat{\sigma}$	50.36	42.96	32.55	37.97	
$\hat{\sigma}_m$	15.92	13.58	10.85	19.42	
n	10	10	9	8	1

Asphalt

AM-17

LT	<u>.69 sec</u>	<u>.83 sec</u>	<u>1.11 sec</u>	<u>2.47 sec</u>	<u>∞</u>
$\bar{F}_x$	782	782	736	730	727
$\hat{\sigma}$	39.34	50.69	20.20	31.56	
$\hat{\sigma}_m$	12.44	16.03	6.38	9.98	
n	10	10	10	10	1

AM-19

LT	<u>.66 sec</u>	<u>1.03 sec</u>	<u>1.53 sec</u>	<u>2.37 sec</u>	<u>∞</u>
$\bar{F}_x$	846	864	848	793	808
$\hat{\sigma}$	34.52	25.99	35.53	29.94	
$\hat{\sigma}_m$	10.91	8.21	12.56	10.58	
n	10	10	8	8	1

BM-13

LT	<u>.67 sec</u>	<u>.86 sec</u>	<u>1.10 sec</u>	<u>2.44 sec</u>	<u>∞</u>
$\bar{F}_x$	628	752	743	731	725
$\hat{\sigma}$	30.96	37.14	48.82	28.89	
$\hat{\sigma}_m$	9.79	11.74	15.43	9.13	
n	10	10	10	10	1

CM-17

LT	<u>.61 sec</u>	<u>.80 sec</u>	<u>1.22 sec</u>	<u>2.31 sec</u>	<u>∞</u>
$\bar{F}_x$	725	765	792	745	740
$\hat{\sigma}$	46.93	31.65	37.36	29.16	
$\hat{\sigma}_m$	20.99	10.00	13.21	10.31	
n	5	10	8	8	1



FM-3

LT	<u>.62 sec</u>	<u>.87 sec</u>	<u>1.27 sec</u>	<u>2.26 sec</u>	<u>∞</u>
$\bar{F}_x$	672	692	658	664	648
$\hat{\sigma}$	57.41	69.05	60.23	50.28	
$\hat{\sigma}_m$	18.16	20.82	19.06	15.91	
n	10	11	10	10	1

ZM-5

LT	<u>.80 sec</u>	<u>1.08 sec</u>	<u>1.66 sec</u>	<u>2.77 sec</u>	<u>∞</u>
$\bar{F}_x$	849	835	813	806	802
$\hat{\sigma}$	34.76	35.19	25.03	14.69	
$\hat{\sigma}_m$	10.99	11.12	7.91	5.19	
n	10	10	10	8	1

## APPENDIX 4

### EXAMPLE OF STATISTICAL PROCEDURES EMPLOYED USING DATA FROM TIRE AM-17 ON CONCRETE

#### A. COCHRAN'S TEST FOR HOMOGENEITY OF VARIANCE [4]

$$\text{Variance} = \hat{\sigma}^2$$

$$C = \frac{\hat{\sigma}_{\max}^2}{4 \sum_{j=1} \hat{\sigma}_j^2}$$

$$C = \frac{(31.91)^2}{(31.91)^2 + (25.14)^2 + (26.94)^2 + 27.09^2} = \frac{1018.24}{3109.89} = .32$$

Critical value of C from tables [4] is .502 for  $\alpha = .05$ , four variances, ten samples per variance. The computed value does not exceed the tabulated value, thus we accept the hypothesis that the population variances are all equal.

#### B. ANOVA [4]

Again we will be comparing a computed statistic to a tabulated value.

$$F = \frac{MS_2}{MS_1}$$

where

$$MS_2 = \frac{n \cdot \sum_{j=1}^k (\bar{x}_j - \bar{x})^2}{k - 1}$$

$$= \frac{10 \cdot [(773-736.75)^2 + (742-736.75)^2 + (717-736.75)^2 + (715-736.75)^2]}{3}$$

$$= 7349.16$$

and

$$MS_1 = \frac{\sum_{j=1}^k \hat{\sigma}_j^2}{k} = \frac{\text{denominator of } C}{k} = \frac{3109.89}{4}$$

$$= 777.47 \quad (\text{since all } n\text{'s are equal})$$

$$F = \frac{7349.16}{777.47} = 9.45$$

The appropriate tabulated value of F is 2.88 [4]. The computed value exceeds this tabulated value, thus we reject the hypothesis that the four "treatments" (lock-up rates) all had an equal effect.

#### C. NEWMAN-KEULS METHOD [4]

This procedure tests for significant differences between pairs of means. The statistic used is

$$q_r = \frac{\bar{F}_{x_i} - \bar{F}_{x_j}}{\sqrt{MS_1/n}}$$

where r is the number of steps two means are apart on an ordered scale. In practice, the expression is re-written to define the difference as

$$\bar{F}_{x_i} - \bar{F}_{x_j} = q_r \sqrt{MS_1/n} \quad *$$

---

\*In cases where the n's are not all equal, a harmonic n should be used;

$$\tilde{n} = \frac{k}{1/n_1 + 1/n_2 + \dots + 1/n_k}$$

and  $q_r$  is obtained from tables.  $MS_1 = 777.47$  as found in part B and  $n = 10$ .

The Newman-Keuls method is best illustrated in the following table of ordered differences.

Treatments		4	3	2	1	r	$q_r \sqrt{MS_1/n}$
	Means	715	717	742	773		
4	715	—	2	27	58	4	33.56
3	717		—	25	56	3	30.48
2	742			—	31	2	25.28
1	773				—	1	

The body of the table contains differences between means. The means are ordered from lowest to highest. Dashed lines connect differences of equal  $r$ ; these differences of equal  $r$  lie on diagonals. ( $r$  is defined such that a mean is "one step" away from itself; thus the smallest practical value of  $r$  is 2.) The values of the critical difference between ordered means for each  $r$ ,  $q_r \sqrt{MS_1/n}$ , are displayed on the right.

$$\sqrt{MS_1/n} = \sqrt{777.47/10} = 8.81$$

$$\left. \begin{aligned} q_4 &= 3.81 \\ q_3 &= 3.46 \\ q_2 &= 2.87 \end{aligned} \right\}$$

obtained from Tables [4] for  $N-k = 36$  degrees of freedom,  $\alpha = .05$ .

Beginning with  $r = 4$ , the difference between means resulting from treatment 1 (the fastest lock-up rate) and treatment 4 (the 2.4-second rate) is 58 which exceeds the critical value of 33.56. Therefore, these two values of  $\bar{F}_x$  are significantly different. For  $r = 3$ , the mean value of treatment 2 is not significantly different from that of treatment 4, but 1 is different from 3; i.e., 27 does not exceed 30.48 but 56 does exceed it. For  $r = 2$ , treatments 3 and 4, and 2 and 3 do not differ significantly while 1 and 2 do. These results may be summarized as follows:

4 3 2 1

symbolizing that the three slower lock-up rates produced mean values of peak braking force that did not differ significantly among themselves but that did all differ from that produced by the fastest lock-up rate.

It was not possible to include the mean value from the steady-state test, treatment 5, in the Newman-Keuls procedure since it is a single specimen. However, since this steady-state value, 720, is well within the  $\pm 2 \hat{\sigma}_m$  limits on the mean value resulting from the 2.4-second test, treatment 4, the two treatments are regarded as not significantly different:

$$\bar{F}_{x_4} - 2\hat{\sigma}_m < \bar{F}_{x_5} < \bar{F}_{x_4} + 2\hat{\sigma}_m$$

$$715 - 17 < 720 < 715 + 17$$

The results for tire AM-17 on concrete can then be summarized  
as

5 4 3 2 1

## PART II

### TIRE-TRACTION GRADING NUMERICS DESCRIPTIVE OF TIRE SIDE-FORCE CHARACTERISTICS

The necessity for obtaining tire quality grading numerics which relate to tire side, or lateral, shear force characteristics derives from the recent finding that the maximum lateral force (MLF) ranking of a tire group shows poor correlation with the maximum braking force (MBF) ranking of the same tire group [1]. Although the correlation of an MLF ranking with an MBF ranking is found to be somewhat dependent on test surface, the experimental evidence indicates that it is insufficient to grade tire traction quality on the basis of tire braking, or longitudinal, force numerics alone. Part II of this report deals with the condensation of free-rolling lateral tire force data into several key numerics which (a) relate to vehicle directional control (viz, small correctional maneuvers and limit-maneuver performance) and (b) rank tires according to three independent lateral traction qualities, viz, (1) cornering stiffness, (2) MLF at a nominal speed and (3) the speed sensitivity of MLF.

The selection rationale and the application of these three side force numerics are discussed below.

#### 2.1 CORNERING STIFFNESS, $C_\alpha$

The cornering stiffness,  $C_\alpha$ , is defined as the negative value of the derivative of lateral shear force,  $F_y$ , with respect to slip angle,  $\alpha$ , viz,

$$C_\alpha \equiv - \left. \frac{dF_y}{d\alpha} \right|_{\substack{\alpha = 0 \\ \text{dry surface} \\ \text{specified load and pressure}}} \quad (1)$$

Although cornering stiffness may be evaluated at any set of operating conditions (e.g., load, pressure, velocity, slip angle, etc.), the above definition, as applied to quality grading purposes, requires that it be evaluated at the origin of the  $F_y$  versus  $\alpha$  data plot as obtained on a dry surface with the tire operated at a specified\* load and pressure.

The rationale for evaluating  $C_\alpha$  at the origin of the  $F_y$  versus  $\alpha$  data plot derives from the experimental evidence indicating that, at small slip angles, the lateral force developed by a tire can be approximated by a linear equation, viz,

$$F_y = - C_\alpha \alpha \quad (2)$$

Equation (2) is a key component in most computer simulations of vehicle dynamic performance which are restricted to small course-correctional maneuvers—such as normal turning maneuvers. This linear relationship between lateral force and small slip angles is also utilized in the analysis of vehicle stability. The cornering stiffness parameter,  $C_\alpha$ , is clearly a crucial numeric which should be included in the set of tire quality grading numerics.

A comparison of mobile tire tester data obtained at 40 mph on two dry surfaces, asphalt and concrete, with flat bed measurements made on the same tires suggests that  $C_\alpha$  is relatively independent of speed and surface. A comparison for a four-tire group, which includes two constructions and three aspect ratios, is given in Table 1.

In examining Table 1, it appears that the slightly higher values of  $C_\alpha$  obtained on the mobile tire tester data may be due

---

\*The specified load and pressure would be the values proposed for longitudinal traction quality grading [2].



TABLE 1

COMPARISON OF CORNERING STIFFNESS VALUES DERIVED FROM FLAT BED DATA AND MOBILE TIRE TESTER DATA OBTAINED AT 40 MPH ON DRY ASPHALT AND DRY CONCRETE TEST SURFACES

		Cornering Stiffness, $C_{\alpha}$ (lb/deg)		
		Test Method:	Mobile (Asphalt)	Mobile (Concrete)
<u>Size</u>	<u>Type</u>	Flat Bed		
F78-14	Belted-Bias	162	177	163
F60-14	Belted-Bias	200	208	187
FR70-14	Radial	175	175	159
FR70-14	Radial	168	172	175

to centrifugal-force stiffening of the tire carcass. Lower (at least ten percent) values of  $C_{\alpha}$  are measured when the same tires are tested at highway speeds on wet surfaces with these reduced values presumably resulting from a decrease in contact length due to water film penetration of the contact patch.

The cornering stiffness,  $C_{\alpha}$ , derived according to Equation (1) with data measured on a dry paved surface, is herein proposed as a tire quality grading numeric which relates entirely to the influence of tire structural characteristics on vehicle directional control. The remainder of this report is concerned with numerics that relate to the frictional performance of a tire-road combination.

## 2.2 MAXIMUM LATERAL FORCE AND ITS SENSITIVITY TO VELOCITY

A recent study of speed gradient data, which involved calculating a number of rank correlations for a group of eleven tires ranked according to each of three braking force values

(maximum braking force, locked wheel braking force, and braking force at 80% lock-up), as measured at one speed, with the same set of tires ranked at a different speed, has concluded that it is insufficient to utilize tire traction grading numerics measured at a single test speed [3]. The referenced study found poor correlation between the various braking force rankings at 20, 40, and 55 mph.

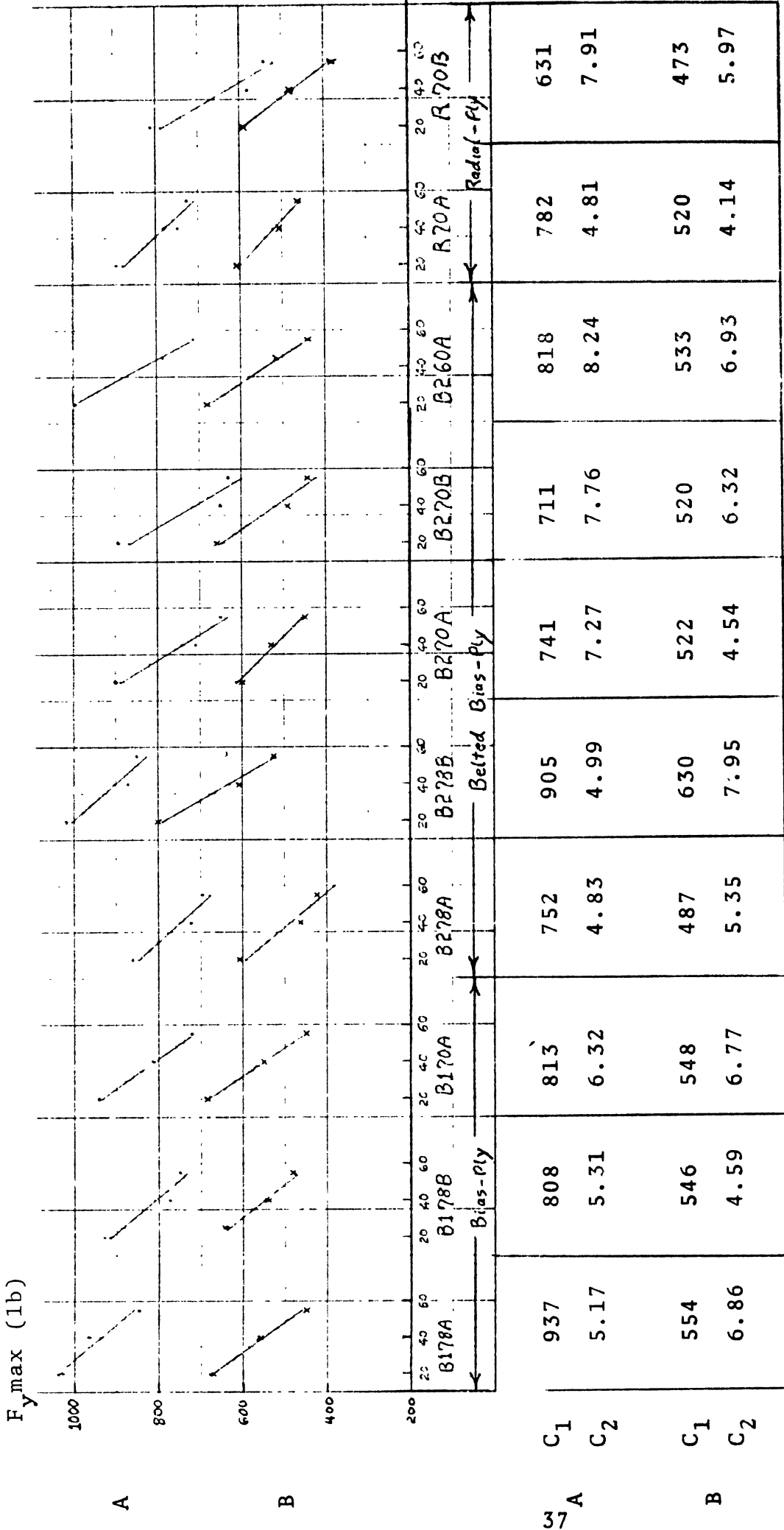
Examination of Figure 1, which shows maximum lateral force data for ten tires at three speeds on two surfaces, indicates that maximum lateral force rankings made at different speeds will also correlate poorly. Apparently, certain aspects of tire construction, most probably the tread pattern, have a substantial influence on the speed sensitivity of maximum lateral force measured on a wet surface. It is also evident, from the data shown in Figure 1, that pavement surface has a measurable influence on the speed sensitivity of maximum lateral force.

The variation of lateral force with velocity has been the subject of numerous wet traction test programs. The test data gathered has invariably indicated a linear decrease of lateral force as tire velocity increases. The rate of decrease is found to depend on many factors and is influenced by pavement surface conditions as well as tire variables.

A theory on the wet cornering traction of free-rolling tires has been proposed by Veith [4]. Veith's theory, which is based on the generally-accepted assumption that elastohydrodynamic lubrication\* prevails over the major portion of the wet traction contact region, predicts the linearity of speed gradient data from the postulate that the fraction of the tire contact area which is in the elastohydrodynamic mode of lubrication is a linear function of speed. This theory, which is really a hypothesis, is well substantiated by the linearity of traction data obtained

---

\*Elastohydrodynamic lubrication refers to the situation where elastic surface deformation plays a significant role in the hydrodynamic lubrication process.



A = Wet Asphalt  
 B = Wet Concrete

$$C_1 = F_y \text{ max at 40 mph}$$

$$C_2 = - \frac{dF_y}{dV} \text{ (slope of linear regression)}$$

Figure 1. Influence of speed on the maximum lateral force developed by 10 tires on two wet surfaces (. asphalt and x concrete). Regression lines shown. Tire load: 1100 lb. Tire pressure: 28 psi.

from tires of different constructions, sizes, tread patterns, and tread compounds. Linear relationships between traction and speed are also found when tires are tested on surfaces of various materials and textures and for tests made in varying depth of water cover. Pottinger and Veith [5] report that well over 500 such plots of lateral force versus velocity have been made. Cornering friction coefficients as low as .04 have been obtained and all evidence to date indicates that traction reduces linearly with speed down to this lower limit.

This above-referenced research is cited as justification for utilizing a minimum number of measurements of maximum lateral force versus speed to ascertain the velocity sensitivity of maximum lateral force. A linear regression analysis has been applied to the speed-gradient data consisting of three data points for each tire (on each surface) as shown in Figure 1. The resulting linear regression lines, as shown in the figure, appear to fit the data extremely well. The poorest regression correlation coefficient found in this analysis exceeded .94 (1.0 indicates that all points lie on a straight line).

Two lateral traction numerics can be derived from this linear regression approximation of maximum lateral force as a function of speed. These numerics, which define the regression line itself, are:

- (1)  $MLF_{40}$  - the maximum lateral force predicted by the regression at 40 mph
- (2)  $\frac{dMLF}{dV}$  - the slope of the speed gradient regression line.

Although any point on the regression line could be used for defining these numerics, it is reasonable to select the speed of 40 mph, this being the velocity proposed for longitudinal traction quality grading [2].

It is convenient to represent the above numerics by the symbols,  $C_1$  and  $C_2$ , respectively, viz,

$$C_1 = \text{MLF}_{40} \quad (3)$$

$$C_2 = \frac{d\text{MLF}}{dV}$$

With these definitions, the equation of the linear speed gradient regression line is

$$\text{MLF}(V) = C_1 + C_2 \cdot (40-V) \quad (4)$$

where  $\text{MLF}(V)$  is the maximum lateral force expressed as a function of velocity.

As tire traction research has not progressed to the point where pavement surface characteristics can be defined, reproduced, and standardized, there is no recourse other than to measure  $C_1$  and  $C_2$  on at least two different surfaces. The test surfaces used should exhibit variation in both material and texture. The asphalt and concrete surfaces proposed for longitudinal traction quality grading [2] are logical choices. The frictional performance variation found on asphalt and concrete surfaces is evident in the data plotted in Figure 1. The variation in frictional performance is quantified by the numerics  $C_1$  and  $C_2$ , listed for both surfaces in Table 2.

### 2.3 INTERPRETATION OF LATERAL TRACTION QUALITY GRADING NUMERICS

The relationship of the lateral traction quality grading numerics,  $C_\alpha$ ,  $C_1$ , and  $C_2$ , to tire properties is elucidated by a study of these numerics listed in Table 2, which were obtained for 10 highway tread F-size tires of various aspect ratios (all on 14-inch rims). All five of the major manufacturers are represented in this tire sample.

TABLE 2

REGRESSION ANALYSIS NUMERICS DERIVED  
FROM DATA SHOWN IN FIGURE 1

		MLF Regression Analysis Data at 40 mph				
		Wet Asphalt		Wet Concrete		
Tire	Code	$C_\alpha$	$MLF_{40}$	$-\frac{dMLF}{dV}$	$MLF_{40}$	$-\frac{dMLF}{dV}$
Bias-Ply	B178A	152	937	5.17	554	6.86
	B178B	157	808	5.31	546	4.59
	B170A	204	813	6.32	548	6.77
Belted Bias-Ply	B278A	134	752	4.83	487	5.35
	B278B	192	905	4.99	630	7.95
	B270A	164	741	7.27	522	4.54
	B270B	193	711	7.76	520	6.32
	B260A	220	818	8.24	533	6.93
Radial	R70A	188	782	4.81	520	4.14
	R70B	187	631	7.91	473	5.97

Tires R70A and R70B are radial-ply FR70-14 tires from two different manufacturers (Firestone and Goodrich). These tires are similar in profile and materials (rayon carcass, rayon belt) but have tread patterns which differ significantly in void percentage. (Tread pattern data are tabulated in Table 3.)

TABLE 3  
TREAD PATTERN DATA FOR TWO RADIAL TIRES

Code	Tread Arc*	Ribs	Groove Depths (in)		Contact Print**	
			Shoulder	Crown	Void (%)	Length (in)
R70A	6.50	5	.40	.36	47.0	7.12
R70B	6.50	7	.40	.34	37.0	7.08

\*Shoulder-to-shoulder transverse arc length (inches, uninflated)

\*\*At test load (1100 lb) and 24 psi. The % void is the percent of noncontact area enclosed by the contact perimeter. Kerfing is included in the void percentage.

In view of the similar construction, profile, and materials, it is expected that the cornering stiffness coefficients,  $C_{\alpha}$ , measured for these two tires should be nearly identical, as was found (viz,  $C_{\alpha} = 188$  and  $187$ ). The frictional performance of these tires on wet surfaces is, however, highly dependent on tread pattern. The more open tread pattern (47% void) employed on tire R70A is responsible for its superior wet traction performance as measured by the numerics  $C_1$  and  $C_2$ . A higher value of  $C_1$  (maximum lateral force at 40 mph) was found for tire R70A on both surfaces. The lower values of  $C_2$ , found for R70A, indicate that the maximum lateral force is less sensitive to speed on these same surfaces.

Although it generally appears that a high maximum lateral force numeric,  $C_1$ , is associated with a high cornering stiffness,  $C_{\alpha}$ , the wet traction performance of a tire is primarily determined by its tread pattern. The interactive influences of cornering stiffness and tread pattern on the maximum lateral force numeric produced by three tires of bias ply construction is evident in Table 4.

TABLE 4

THE INFLUENCE OF TREAD PATTERN AND CORNERING STIFFNESS  
ON MAXIMUM LATERAL FORCE PRODUCED BY THREE BIAS-PLY TIRES

Tire Code	Tire Size	Pattern Void (%)	$C_{\alpha}$	Wet. Asphalt Wet Concrete	
				$C_1$	$C_1$
B178A	F78-14	45.0	152	937	554
B178B	F78-14	36.3	157	808	546
B170A	F70-14	31.4	204	813	548

The first two tires listed in Table 4 have nearly the same cornering stiffness, as may be expected from their identical size and similar materials (both have polyester carcass). The more open tread pattern on tire B178A (45% void) appears to have enabled this tire to produce substantially higher (in comparison to the force produced by tire B178B) maximum lateral force on the wet asphalt surface.\* The third tire (B170A) has a substantially higher  $C_{\alpha}$ , probably due to its wider profile, and thus produces maximum lateral forces comparable to the forces produced by tire B178B, even though the percent void is substantially less.

Similar behavior is evident for the tires of belted-bias construction which are grouped in Table 5. It is seen here, also, that higher cornering stiffness,  $C_{\alpha}$ , is associated with higher maximum lateral force,  $C_1$ , unless the tread pattern has a low void percentage. Tire B278B, which couples a high cornering stiffness with a high void percentage, produces substantially higher maximum lateral force on both surfaces than any of the

\*The two test surfaces are very similar in texture, possessing a slight macro- and moderate microtexture. Nonetheless, the open tread pattern of the B178A tire was apparently more effective on the asphalt than on the concrete surface.



TABLE 5

THE INFLUENCE OF TREAD PATTERN AND CORNERING STIFFNESS  
ON MAXIMUM LATERAL FORCE PRODUCED BY FIVE BELTED-BIAS TIRES\*

Tire Code	Tire Size	Pattern Void (%)	$C_{\alpha}$	Wet Asphalt	Wet Concrete
				$C_1$	$C_1$
B278A	F78-14	40.6	134	752	487
B278B	F78-14	39.3	192	905	630
B270A	F70-14	37.4	164	741	522
B270B	F70-14	32.0	193	711	520
B260A	F60-14	42.7	220	818	533

\*These tires all have a polyester carcass and a fiberglass belt.

other tires, including tire B260A which also exhibits high cornering stiffness and high void percentage. Referring back to Table 2, it is seen that tire B260A also has a high speed gradient numeric,  $C_2$ , on both surfaces which may partially explain why this tire does not produce exceptionally high maximum forces even though the void percentage and cornering stiffness numerics are high.

It is difficult to relate the speed gradient numeric,  $C_2$ , to tire construction and profile. Apparently, this numeric cannot be as easily controlled as  $C_1$  by adjustments in tread pattern and cornering stiffness.

Finally, to show that the proposed lateral traction quality grading numerics are independent measures, rank correlation coefficients were computed for the 10 tires (of Table 2) ranked according to favorable behavior as indicated by these measures. Table 6 lists the rank correlation coefficients found. The low absolute values of these correlation coefficients indicate that  $C_{\alpha}$ ,  $C_1$ , and  $C_2$  are indeed independent measures of tire performance.

TABLE 6

RANK CORRELATION COEFFICIENTS FOR 10 TIRES RANKED  
ACCORDING TO LATERAL TRACTION MEASURES  $C_\alpha$ ,  $C_1$ ,  $C_2$

<u>Measures</u>	<u>Rank Correlation Coefficient</u>	
	<u>Asphalt</u>	<u>Concrete</u>
$C_\alpha$ vs. $C_1$	+ .103	+ .179
$C_\alpha$ vs. $C_2$	- .491	- .442
$C_1$ vs. $C_2$	+ .297	- .585

## REFERENCES

1. Neill, A.H., Jr. and Boyd, P.L., "Research on Wet Tire Traction," Tire Science and Technology, Vol. 1, No. 2, May 1973, pp. 172-189.
2. National Highway Traffic Safety Administration, "Uniform Tire Quality Grading," Federal Register, Vol. 39, No. 116, June 14, 1974, pp. 20808-20813.
3. Tielking, J.T., "Analysis and Report of Speed Gradient Data," UM-HSRI-PF-73-7. Sponsored by the Safety Systems Laboratory of NHTSA, Nov. 1973.
4. Veith, A.G., "Measurement of Wet Cornering Traction of Tires," Rubber Chemistry and Technology, Vol. 44, No. 4, Sept. 1971, pp. 962-995.
5. Veith, A.G. and Pottinger, M.G., "Tire Wet Traction: Operational Severity and It's Influence on Performance," Presented at Symposium on Physics of Tire Traction, General Motors Research Laboratories, Warren, Mich., Oct. 8-9, 1973.

